Oxidation products of 5-methyl cytosine are decreased in senescent cells and tissues of progeroid mice

Ewelina Zarakowska, PhD,[1†], Jolanta Czerwinska, MSc,[2†], Agnieszka Tupalska, MSc,[3], Matt J. Yousefzadeh, PhD,[4], Siobhán Q. Gregg, PhD,[5], Claudette M. St. Croix, PhD,[5], Laura J. Niedernhofer, MD, PhD,[4], Marek Foksinski, PhD,[1], Daniel Gackowski, PhD,[1], Anna Szpila, PhD,[1], Marta Starczak, MSc,[1], Barbara Tudek, Prof.,[2,3], Ryszard Olinski, Prof.,[1*]

[1]Department of Clinical Biochemistry, Faculty of Pharmacy, Collegium Medicum in Bydgoszcz, Nicolaus Copernicus University in Toruń, Karlowicza 24, 85-092 Bydgoszcz, Poland

[2]Institute of Biochemistry and Biophysics, Polish Academy of Sciences, Pawinskiego 5a, 02-106 Warsaw, Poland

[3]Institute of Genetics and Biotechnology, Faculty of Biology, University of Warsaw, Pawinskiego 5a, 02-106 Warsaw, Poland

[4]Department of Molecular Medicine, Center on Aging, The Scripps Research Institute, Jupiter, FL 33458 USA

[5]Department of Cell Biology, University of Pittsburgh, Pittsburgh, PA 15261, USA

†These authors contributed equally to this manuscript.

Address correspondence to Ryszard Olinski, Department of Clinical Biochemistry, Faculty of Pharmacy, Collegium Medicum in Bydgoszcz, Nicolaus Copernicus University in Toruń, Karlowicza 24, 85-092 Bydgoszcz, Poland. E-mail: ryszardo@cm.umk.pl

Correspondence may also be addressed to

Barbara Tudek, Institute of Biochemistry and Biophysics, Polish Academy of Sciences, Pawinskiego 5a, 02-106 Warsaw, Poland. E-mail: tudek@ibb.waw.pl

Abstract

5-Hydroxymethylcytosine and 5-formylcytosine are stable DNA base modifications generated from 5-methylcytosine by the ten-eleven translocation protein family that function as epigenetic markers. 5-Hydroxymethyluracil may also be generated from thymine by ten-eleven translocation enzymes. Here, we asked if these epigenetic changes accumulate in senescent cells, since they are thought to be inversely correlated with proliferation. Testing this in ERCC1-XPF-deficient cells and mice also enabled discovery if these DNA base changes are repaired by nucleotide excision repair. Epigenetic marks were measured in proliferating, quiescent and senescent wild-type and *Ercc1*$^{-/-}$ primary mouse embryonic fibroblasts. The pattern of epigenetic marks depended more on the proliferation status of the cells than their DNA repair capacity. The cytosine modifications were all decreased in senescent cells compared to quiescent or proliferating cells, whereas 5-(hydroxymethyl)-2'-deoxyuridine was increased. *In vivo,* both 5-(hydroxymethyl)-2'-deoxyuridine and 5-(hydroxymethyl)-2'-deoxycytidine were significantly increased in liver tissues of aged wild-type mice compared to young adult wild-type mice. Livers of *Ercc1*-deficient mice with premature senescence and aging had reduced level of 5-(hydroxymethyl)-2'-deoxycytidine and 5-formyl-2'-deoxycytidine compared to aged-matched wild-type controls. Taken together, we demonstrate for the first time, that 5-(hydroxymethyl)-2'-deoxycytidine is significantly reduced in senescent cells and tissue, potentially yielding a novel marker of senescence.

Keywords: 5-hydroxymethylcytosine, 5-formylcytosine, 5-hydroxymethyluracil, ERCC1-XPF endonuclease, aging

Introduction

Cytosine methylation, usually at CpG dinucleotides, is one of the most important epigenetic modifications and has a profound impact on gene repression, cellular identity and organismal fate (1). The reversion of DNA methylation (demethylation) is equally important to activate previously silenced genes, and mounting evidence suggests that replication-independent enzymatic demethylation or oxidation are important processes in the function of somatic cells (2).

The most plausible mechanisms of active DNA demethylation/iterative oxidation involve ten-eleven translocation (TET) proteins that catalyze oxidation of 5-methylcytosine (5-mCyt) to 5-hydroxymethylcytosine (5-hmCyt), which can be further oxidized to 5-formylcytosine (5-fCyt) and 5-carboxycytosine (5-caCyt). In addition, there is experimental evidence that 5-hydroxymethyluracil (5-hmUra) may also be generated by TET enzymes from thymine and has epigenetic functions ((3), for review see: (4)).

5-hmCyt is enriched in a subset of promoters and enhancers of actively transcribed genes (5). Moreover, all of these DNA modifications recruit proteins involved in DNA repair and in chromatin remodelling, as well as in transcription (3,6). ERCC1-XPF is a DNA repair endonuclease required for nucleotide excision repair (NER) (7), which may help remove modified pyrimidines. Low expression of ERCC1-XPF promotes accelerated aging of humans and mice (8) caused by faster accumulation of endogenous DNA damage and senescent cells (9). Senescent cells have been demonstrated to play a direct causal role in aging (10,11). It was also demonstrated that ERCC1-XPF may be involved in transcription initiation-dependent chromatin modification linked to DNA demethylation (12). All these observations prompted us to ask whether there are differences in epigenetic DNA modifications between *Ercc1*$^{-/-}$ and wild-type (WT) cells and whether there are characteristic features of senescent cells in terms of epigenetic marks.

We measured the level of the whole spectrum of recently discovered epigenetic marks, *i.e.* 5-methyl-2'-deoxycytidine (5-mdC), 5-(hydroxymethyl)-2'-deoxycytidine (5-hmdC), 5-formyl-2'-deoxycytidine (5-fdC), 5-carboxy-2'-deoxycytidine (5-cadC), 5-(hydroxymethyl)-2'-deoxyuridine (5-hmdU) in: (i) replicating, quiescent (growth arrested) and senescent wild-type and *Ercc1*$^{-/-}$ cells and (ii) in the liver of wild-type and *Ercc1*-deficient mice, during physiological and accelerated aging, respectively. To measure all of the modifications above, we applied a recently developed rapid, specific, and sensitive isotope-dilution automated online two-dimensional ultra-performance liquid chromatography with tandem mass spectrometry (2D-UPLC-MS/MS) (13).

Methods

Generation and culture of primary mouse embryonic fibroblasts (MEFs)

Ercc1$^{-/-}$ primary MEFs were prepared from day 13 embryos derived from crossing inbred C57BL/6J mice heterozygous for an *Ercc1* null allele, as previously described (14). MEFs were simultaneously derived from WT littermate embryos for use as controls. Primary MEFs were cultured in a 1:1 mixture of Dulbecco's modified Eagle's medium and Ham's F10 with 10% fetal bovine serum, non-essential amino acids and antibiotics, and incubated at 3% O_2. Three independent MEF lines of each genotype were used for experiments. Cells from each embryo were split onto three dishes at passage 1 (p1). One plate was harvested at passage 2 when 75% confluent (P2 replicative). The second was passaged to 100% confluence then left for 48 hours (P2 quiescent). The third was passaged to passage 7 (p7) where it only reached 50% confluence (P7 senescent). Cells were harvested, washed in PBS, and snap frozen in liquid nitrogen and stored at -80°C until analysis.

Animals

Ercc1$^{-/\Delta}$ mice were generated by breeding *Ercc1*$^{+/-}$ and *Ercc1*$^{+/\Delta}$ mice in inbred C57Bl/6J and FVB/n backgrounds, respectively, to create a cohort of mice that were in an f1 hybrid

background yet genetically identical. The mice were genotyped by PCR as previously described (14). WT littermates were used as controls. Aged WT mice were bred in house and were in the same f1 genetic background. Animal husbandry and experimental procedures were approved by The Scripps Research Institute Florida IACUC.

Measurement of epigenetic marks

DNA extraction and DNA hydrolysis to deoxynucleosides (dN) was performed using a method described previously (13). The 2D-UPLC–MS/MS analyses were performed as describe (13). Briefly, DNA hydrolysates were spiked with a mixture of internal standards in volumetric ratio 4:1, to concentration of 50 fmols/µL of [D_3]-5-hmdC, [$^{13}C_{10}$, $^{15}N_2$]-5-fdC, [$^{13}C_{10}$, $^{15}N_2$]-5-cadC and [$^{13}C_{10}$, $^{15}N_2$]-5-hmdU. Chromatographic separation was performed with a Waters Acquity 2D-UPLC system with photo-diode array detector, for the first-dimension chromatography (used for quantification of unmodified dN and 5-mdC), and Xevo TQ-S tandem quadrupole mass spectrometer for second dimension chromatography. At-column-dilution technique was used between first and second dimension for improving retention on the trap/transfer column. The columns used were: a Phenomenex Kinetex C-18 column (150 mm×2.1 mm, 1.7 µm) at the first dimension, a Waters X-select C18 CSH (100 mm×2.1 mm, 1.7 µm) at the second dimension and Waters X-select C18 CSH (30 mm×2.1 mm, 1,7 µm) as trap/transfer column. The chromatographic system was operated in heart-cutting mode, indicating that selected parts of the effluent from the first dimension were directed to trap/transfer column via 6-port valve switching, which served as the “injector” for the second-dimension chromatography system. The flow rate at the first dimension was 0.25 mL/min and the injection volume was 0.5-2 µL. The separation was performed with a gradient elution for 10 min using a mobile phase 0.1% acetate (A) and acetonitrile (B) escalating from 1-5% B over 5 min. The column was then washed with 30% acetonitrile and re-equilibrated with 99% A for 3.6 min. The flow rate at the second dimension was 0.35 mL/min. The separation was performed with a gradient elution for

10 min using a mobile phase 0.01% acetate (A) and methanol (B) ramping from 1-50% B over 4 min, followed by isocratic flow of 50% B for 1.5 min then re-equilibration with 99% A until the next injection. All samples were analyzed in three to five technical replicates of which technical mean was used for further calculation. Mass spectrometric detection was performed using the Waters Xevo TQ-S tandem quadrupole mass spectrometer, equipped with an electrospray ionization source. Collision-induced dissociation was obtained using argon 6.0 at 3 x 10^{-6} bar pressure as the collision gas. Transition patterns for all the analyzed compounds, as well as specific detector settings were determined using the MassLynx 4.1 Intelli-Start feature.

RNA isolation and qPCR

Total RNA was isolated from MEFs using RNeasy isolation kit (Qiagen, Valencia, CA). Total RNA was quantified using a Nanodrop spectrophotometer (Thermo Fisher, Waltham, MA) and 1 μg of total RNA was used to generate cDNA with the Transcriptor First Strand cDNA synthesis kit (Roche, Basel Switzerland) according to the manufacturer's specification. Gene expression changes in *Gapdh*, $p16^{Ink4a}$, and $p21^{Cip1}$ were quantified by qPCR reactions using 20 μL reaction volumes using a StepOne thermocycler (Thermo Fisher, Waltham, MA) with input of 50 ng total RNA per reaction except for $p16^{Ink4a}$ (100 ng). Reactions were performed in duplicate in three separate experiments. Data was analyzed by ΔΔCt method and expression was normalized to *Gapdh*. qPCR primer sequences are listed in Supplementary Table 1.

Immunofluorescence

WT and $Ercc1^{-/-}$ MEFs were cultured on glass coverslips until they reached 50% confluence. Cells were fixed with 2% paraformaldehyde in PBS for 15 min. Cells were permeabilized with 0.1% Triton X-100 in PBS and the phosphorylated form of γH2AX detected with monoclonal anti-γH2AX (05-636, Millipore, Billerica, MA) and Alexa 594-conjugated goat anti-mouse IgG (A-11005, Invitrogen, Carlsbad, CA) in PBS with 0.15% glycine and 0.5% bovine serum albumin. γH2AX foci were counted with an Olympus BX51 fluorescent microscope.

Senescence-associated β-Galactosidase (SA-β-Gal) staining

Frozen tissue sections and primary WT and *Ercc1*$^{-/-}$ MEFs were fixed in 0.25% glutaraldehyde and 2% paraformaldehyde for ten min at room temperature. Following three rinses in PBS, SA-β-Gal staining was performed as previously described (15,16).

Immunoblotting

Cells were trypsinized, pelleted, and the pellet was dissolved in ice-cold NETT buffer (100mM NaCl, 50mM Tris pH 7.5, 5mM EDTA pH 8.0, 0.5% Triton-X) with Mini-complete protease inhibitor tablet (11836153001, Roche Applied Science, Indianapolis, IN). Fifty µg of whole cell lysate was boiled in 4xloading buffer [0.25M Tris-HCl (pH 8.5), 8% SDS, 1.6mM EDTA, 0.1M DTT, 0.04% bromophenol blue, 40% glycerol] and separated by SDS-PAGE on a 4-20% Mini-PROTEAN gradient gel (Bio-Rad, Hercules, CA), and transferred to nitrocellulose membrane. Primary antibodies against p16 (clone M-156, Santa Cruz Biotechnology, Santa Cruz, CA), beta-actin (ab13822, Abcam, Cambridge, MA) were used at a dilution of 1:500. This was followed by a 1:1000 dilution of either AP-conjugated anti-chicken IgG (ab6878, Abcam, Cambridge, MA) or AP-conjugated anti-rabbit IgG (S-373, Promega, Madison, WI). Blots were developed and imaged using the Alpha Innotech Red gel imaging system. Densitometry was calculated using the spot density software on the Alpha Innotech Red gel imaging system.

Statistical analysis

Statistical analysis was performed using STATISTICA version 13 (www.statsoft.com). Repeated-measures analysis of variance (ANOVA)-LSD test was performed to assess the differences in the levels of epigenetic DNA modifications. In all analyzes $p<0.05$ was considered statistically significant. The results are depicted in the graphs in the form of average value with standard deviation.

Results

Epigenetic marks in replicative-, quiescent- and senescent cells

5-MdC, 5-hmdC, 5-fdC, and 5-hmdU levels were measured in the genomic DNA isolated from replicative, quiescent and senescent cells. Replicative cells were early passage primary MEFs maintained at 50% confluence. Quiescent cells were early passage primary MEFs maintained at 100% confluence without passaging. Senescent cells are late passage primary cells (p7). All three were derived from the same embryo and three biological replicates prepared.

Expression of senescence markers $p16^{Ink4a}$ and $p21^{Cip1}$ were measured in the same cells used for methylated and oxidized deoxynucleosides. mRNA levels for both senescence markers were significantly elevated in late passage cells compared to early passage (Figure 1A). Furthermore, expression was elevated in *Ercc1*$^{-/-}$ cells compared to WT. Deletion of *Ercc1* causes reduced expression of the DNA repair enzyme ERCC1-XPF (8), required for NER, interestrand crosslink repair and the repair of some double-strand breaks (17). Deficiency of ERCC1-XPF causes the accumulation of endogenous oxidative DNA damage *in vivo* (18). Thus, *Ercc1*$^{-/-}$ cells have increased expression of senescence markers compared to WT controls.

To confirm premature senescence in *Ercc1*$^{-/-}$ MEFs compared to WT cells, additional markers of cellular senescence in primary MEFs serially passaged at 3% O_2 or 20% O_2, which accelerates senescence of primary MEFs in particular if DNA repair is impaired genetically (19). Three markers of senescence were measured in congenic wild-type and *Ercc1*$^{-/-}$ MEFs at multiple passage numbers: γH2AX foci, SA-β-gal activity and p16 protein levels. With increasing passage of all four cultures, there was a significant increase in the fraction of cells with γH2AX foci (Figure 1B and Supplementary Figure 1). Furthermore, there was a significantly greater fraction of WT and *Ercc1*$^{-/-}$ MEFs with γH2AX foci in cultures grown at 20% O_2 compared to 3% O_2. *Ercc1*$^{-/-}$ MEFs had significantly more γH2AX foci than WT MEFs whether grown at 20% or 3% O_2. SA-β-gal activity is another hallmark feature of senescent

cells (15). SA-β-gal activity followed a very similar pattern as that of γH2AX foci (Figure 1C and Supplementary Figure 1). The fraction of cells staining positively for SA-β-gal increased with increasing passage number in WT and *Ercc1*$^{-/-}$ MEFs, and to a greater extent in cells cultured at 20% O_2 relative to 3%. Significantly more *Ercc1*$^{-/-}$ MEFs stained positively for SA-β-gal at each passage (3, 5 and 7) at 20% O_2, but not until passage 7 if the cells were grown at 3% O_2. The fraction of cells that stained positively for SA-β-gal in any given culture was consistently lower than the fraction staining positively for γH2AX foci.

At passage 3, after only 10-12 days *ex vivo*, the expression of p16 expression was approximately 2-fold higher in *Ercc1*$^{-/-}$ MEFs compared to WT MEFs, when cultured at 3% or 20% O_2 (Figure 1D). p16 expression was also modestly increased in WT cells grown at 20% O_2 compared to 3%, consistent with the other senescence markers. Taken together, these results demonstrate that DNA repair-deficient *Ercc1*$^{-/-}$ primary MEFs undergo cellular senescence more rapidly than congenic WT cells and therefore in our experiments there is likely an increased fraction of senescence cells in the *Ercc1*$^{-/-}$ p7 cultures used to measure DNA methylation relative to WT cultures (Figure 1A and D).

The mean value of 5-mdC in wild-type replicative cells was 8.74/10^3dN (SD±0.3075) (Figure 2A). The level of 5-mdC was not significantly different between WT replicative and quiescent (8.58/10^3dN±0.2795) or senescent cells (8.24/10^3dN±0.6610). However, it is notable that there was a large standard deviation in measurements of 5-mdC in WT senescent cells. Increased heterogeneity is typical of senescent cells (20). The level of 5-mdC was similar between replicative and quiescent *Ercc1*$^{-/-}$ and WT fibroblasts (Figure 2A). This strongly suggests that 5-mdC is not repaired by NER, an ERCC1-dependent repair pathway, consistent with findings of others (21). The levels of 5-mdC was, however significantly lower in senescent *Ercc1*$^{-/-}$ cells (8.07/10^3dN±0.0661) compared to replicative (8.99/10^3dN±0.0525) or quiescent (8.93/10^3dN±0.0251) cells. This likely reflects the fact that in the *Ercc1*$^{-/-}$ cells senescence

more rapidly than WT cells [(8) and Figure 1] and therefore may have additional epigenetic changes (20,22).

For 5-hmdC, the results were more complex (Figure 2B). There was a significant-difference in levels of 5-hmdC between WT and *Ercc1*$^{-/-}$ cells in the replicative and senescent cell populations, but not the quiescent cells. The mutant cells had significantly higher levels of 5-hmdC than WT cells in two of three cell populations, which may reflect an inability to repair these modified bases in the absence of NER. The level of 5-hmdC was similar for both genotypes in quiescent cells, which were $0.04/10^3$dN±0.0054 and $0.04/10^3$dN±0.0026 for the WT and mutant cells respectively. This is consistent with global NER being attenuated in post-mitotic, quiescent cells (23). The highest level of 5-hmdC was observed in quiescent cells, while in senescent cells, the levels were at least 2-fold lower (Table 1). Levels in replicative cells were intermediate. This may indicate reduced TET activity in senescent cells.

We also observed reduced levels of 5-fdC in senescent cells irrespective of genotype (Figure 2C). The highest level of 5-fdC was observed in replicating WT cells (mean value $0.07/10^6$dN±0.0036). This was significantly greater than in *Ercc1*$^{-/-}$ MEFs (mean value $0.05/10^6$dN±0.0040). This may reflect the fact that *Ercc1*$^{-/-}$ primary cells proliferate more slowly than isogenic WT cells. The levels of 5-fdC was reduced in quiescent and senescent cells compared to replicative, regardless of the genotype of the cells (Table 1). Therefore, the levels of 5-fdC appear to correlate best with ability to replicate.

Determination of 5-hmdU revealed a significantly higher level in *Ercc1*$^{-/-}$ senescent cells (mean value $1.14/10^6$dN±0.1165) compared to replicative and quiescent cells, with mean values $0.72/10^6$dN±0.2079 and $0.58/10^6$dN±0.0543, respectively (Figure 2D). There were no significant differences in the level of 5-fdC in WT cells of different replicative capacity (Table 1). 5-cadC was undetectable in primary MEFs, with the limit of detection for this modification being a modification per 10^9 deoxynucleosides in our assay.

Epigenetic marks in mouse tissues

We previously demonstrated that several markers of senescence are more apparent in *Ercc1*$^{-/\Delta}$ mice compared to age-matched littermates (9). This includes reduced hepatocyte proliferation (reduced Ki67 staining post-partial hepatectomy), increased SA-β-gal staining and increased lipofuscin. The same markers are more apparent in livers of aged WT mice compared to young adult animals (9). Hence, we focused on liver for measurement of epigenetic marks.

The profile of epigenetics marks was estimated in DNA isolated from livers of 10-, 15- and 130-week-old WT mice, as well as 10- and 15-week-old DNA-deficient progeroid *Ercc1*$^{-/\Delta}$ mice. The level of 5-mdC was similar in livers of WT mice at all ages (Table 2, Figure 3A). We did not find any significant genotype-specific or age-related differences in the level of 5-mdC in liver tissue.

In contrast, the level of 5-hmdC increased significantly with aging in WT mice (Figure 3B), from $0.34/10^3$dN±0.0175 to $0.78/10^3$dN±0.0058 respectively with $p<0.00001$. 5-hmdC levels were 1.5 fold higher in 10- and 15-week-old WT mouse liver compared to age-matched *Ercc1*$^{-/\Delta}$ mice (Table 2). Nevertheless, there was a significant increase in the level of 5-hmdC in liver of *Ercc1*$^{-/\Delta}$ from 10 to 15 weeks of age, reflecting an age-related increase, similar to WT mice, albeit more accelerated.

5-FdC was detected in all liver tissues analyzed (Figure 3C). There was no significant change in 5-fdC levels in WT mice with aging. However, there was a significant increase in *Ercc1*$^{-/\Delta}$ mice between 10-15 weeks of age (Table 2). Levels of 5-fdC were significantly lower (~1.6-fold) in *Ercc1*$^{-/\Delta}$ mice, compared to WT mice at both ages of mice.

There was no statistically significant difference in the 5-cadC level among 10- ,15- and 130-week-old WT and *Ercc1*$^{-/\Delta}$ mice (Table 2, Figure 3D). The levels 5-hmdU in DNA from 10 week old WT mouse liver reached the value of $0.21/10^6$dN±0.027 (Figure 3E). The level increased significantly to $0.37/10^6$dN±0.038) in old WT mice. There was no significant

difference in 5-hmdU levels between WT and DNA repair- deficient mice at any age tested (Table 2).

Discussion

Fundamental mechanisms that drive aging are poorly understood (reviewed in (24)). However, it is abundantly clear that damaged, senescent cells accumulate as organisms age (16,25-28). Recent studies demonstrate that the clearance of senescent cells in aged mice improves healthspan, thereby establishing that senescence drives multiple age-related pathologies (10,29,30).

Senescence is an irreversible cell cycle arrest that occurs in response to cellular stress (31). Senescence is a genetically programmed tumor suppressor mechanism. DNA damage, which drives mutation accumulation in replicating cells, is a potent driver of senescence (32). Senescent cells remain metabolically active and secrete numerous cytokines, chemokines and matrix remodeling enzymes. Thus, gene expression patterns are altered in senescent cells. Here, we sought to determine if globally, epigenetic changes to DNA are altered in senescent cells by measuring modified pyrimidines in senescent cells compared to quiescent cells in which the cell cycle is reversibly arrested. Late passage, senescent cells had increased expression of p16, increased γH2AX foci, and increased SA-β-Gal activity compared to early passage cells (Figure 1) and this was even more exaggerated in DNA repair deficient *Ercc1*$^{-/-}$ cells. Generally speaking, replicative and quiescent cells were more similar to one another than to senescent cells (Table 1). 5-mdC, 5-hmdC and 5-fdC tended to be lower in senescent cells than non-irreversibly arrested cells, while 5-hmdU tended to be higher. This is consistent with and extends previous work indicating that 5-mdC levels are decreased in senescent or late passage mammalian cells (22,33). Notably, none of the modified pyrimidines were consistently increased in ERCC1-XPF deficient cells and tissue. Hence, there is no reason to believe that any of these modified nucleosides are removed from the genome by nucleotide excision repair.

Recently it was demonstrated that 5-hmCyt is a relatively stable DNA modification and that levels of this modification differ dramatically between various tissues in the mouse, with proliferative tissues having the lowest levels (34,35). In agreement with this, we found that proliferating cells had significantly decreased 5-hmdC compared to quiescent cells (Figure 2B). Intriguingly, the level of 5-hmdC was also 4-fold lower in senescent WT cells compared to quiescent cells. This was replicated in *Ercc1*$^{-/-}$ primary MEFs, suggesting that low levels of 5-hmdC might be a consistent hallmark of senescent cells.

Because of the close ties between senescence and aging (36), we also measured these epigenetic marks in tissues from aged WT and progeroid *Ercc1*-deficient mice, using liver, where senescent cells accumulate as organisms age, as documented by reduced proliferative capacity, increased SA-β-Gal activity, lipofuscin and expression of *p16*^{Ink4a} (9). *In vivo*, 5-mdC and 5-fdC levels did not change with normal aging (Table 2 and Figure 3C), as previously reported for mouse kidney and brain (37). In contrast, 5-hmdC and 5-hmdU were significantly increased in liver of old mice (Figure 3B and E). This is in agreement with a previous study demonstrating an increase in 5-hmdC in brain and kidney of mice with age (37). In contrast, in *Ercc1*-deficient mice, 5-hmdC levels were 1.5-fold lower than age-matched WT mice and 3-fold lower than old WT mice (Figure 3B), which is in keeping with our observation that 5-hmdC is decreased in senescent cells. The difference between the progeroid *Ercc1*$^{-/\Delta}$ and aged WT mice could reflect the fact that there is significantly more oxidative DNA damage in liver of *Ercc1*$^{-/\Delta}$ mice than old WT mice (18), which is a potent driver of cellular senescence (36). Alternatively, *Ercc1*$^{-/\Delta}$ mice display hypercholesterolemia and low triglycerides, while old WT mice do not (9). Thus, it is possible that metabolic differences dictate the differences in 5-hmdC levels between the progeroid and naturally aged mice. Interestingly, decreased levels of 5-hmdC and TET1 expression was recently reported in Down syndrome, which is characterized

by premature aging and senescence (38). Similarly, Xiong et al., reported a significant decline in 5-hmdC levels in human peripheral blood cells with age (39).

It is becoming increasingly clear that the product of 5-mdC oxidation (5-hmdC) may act as an intermediate of active DNA demethylation and play a regulatory role, e.g. controlling the transition between different cell states (40) by bind gene regulatory proteins (41). Therefore, a decrease in this modification in senescent cells may be one of the factors responsible for perturbation of cellular metabolism. It is noteworthy that TET proteins preferentially bind transcription start sites (42), and 5-hmCyt enrichment is found at promoters and enhancers of actively transcribed genes (5,43).

Several recent studies demonstrate that 5-hmCyt is reduced in many types of human malignancies compared to non-malignant tissue (44,45). Interestingly, senescent cells share many things in common with cancer cells, including alteration in gene expression that favors cell survival (29,30,46).

It is unclear why 5-hmCyt is decreased in cancer and in senescent cells. There are several metabolites, including intermediates of the TCA cycle 2-OH-glutarate, succinate and fumarate that inhibit 2-ketoglutarate-dependent dioxygenases, among them the TET enzymes (47). These metabolites may accumulate as a result of metabolic changes that accompany cellular senescence (48). The low levels of 5-hmdC in senescent cells and tissues of mice with a high burden of senescent cells strengthens the similarity between senescent and malignant cells, and may serve as a marker of irreversibly damaged cells.

Supplementary Material

Supplementary data is available at *The Journals of Gerontology, series A: Biological Sciences and Medical Sciences* online.

Funding

This work was supported by the National Science Centre (grant number DEC-2012/07/B/NZ1/00008 (R.O.), http://www.ncn.gov.pl, and Ministry of Science and Higher Education, grant number N N303 819540 (B.T.). L.J.N. and M.J.Y. and C.M.S. were supported by NIH/NIA P01 AG043376. J.C. was supported by the Human Capital Operational Programme 1/POKL/4.3/2012 "Modern Methods, Medicines and Treatments from the Viewpoint of Healthcare and Economy in the 21st-Century Europe – Interdisciplinary Education in Biomedical Sciences, 2nd and 3rd Cycle Studies".

References

(1) Feng S, Jacobsen SE, Reik W. Epigenetic reprogramming in plant and animal development. *Science.* 2010;330:622-627. doi: 10.1126/science.1190614.

(2) Bhutani N, Burns DM, Blau HM. DNA demethylation dynamics. *Cell.* 2011;146:866-872. doi: 10.1016/j.cell.2011.08.042.

(3) Pfaffeneder T, Spada F, Wagner M, et al. Tet oxidizes thymine to 5-hydroxymethyluracil in mouse embryonic stem cell DNA. *Nat Chem Biol.* 2014;10:574-581. doi: 10.1038/nchembio.1532.

(4) Olinski R, Starczak M, Gackowski D. Enigmatic 5-hydroxymethyluracil: Oxidatively modified base, epigenetic mark or both? *Mutat Res Rev Mutat Res.* 2016;767:59-66. doi: 10.1016/j.mrrev.2016.02.001.

(5) Pastor WA, Aravind L, Rao A. TETonic shift: biological roles of TET proteins in DNA demethylation and transcription. *Nat Rev Mol Cell Biol.* 2013;14:341-356. doi: 10.1038/nrm3589.

(6) Iurlaro M, Ficz G, Oxley D, et al. A screen for hydroxymethylcytosine and formylcytosine binding proteins suggests functions in transcription and chromatin regulation. *Genome Biol.* 2013;14:R119. doi: 10.1186/gb-2013-14-10-r119.

(7) Sijbers AM, de Laat WL, Ariza RR, et al. Xeroderma pigmentosum group F caused by a defect in a structure-specific DNA repair endonuclease. *Cell.* 1996;86:811-822. doi:10.1016/S0092-8674(00)80155-5.

(8) Niedernhofer LJ, Garinis GA, Raams A, et al. A new progeroid syndrome reveals that genotoxic stress suppresses the somatotroph axis. *Nature.* 2006;444:1038-1043. doi: 10.1038/nature05456.

(9) Gregg SQ, Gutierrez V, Robinson AR, et al. A mouse model of accelerated liver aging caused by a defect in DNA repair. *Hepatology.* 2012;55:609-621. doi: 10.1002/hep.24713.

(10) Baker DJ, Childs BG, Durik M, et al. Naturally occurring p16(Ink4a)-positive cells shorten healthy lifespan. *Nature.* 2016;530:184-189. doi: 10.1038/nature16932.

(11) Calhoun C, Shivshankar P, Saker M, et al. Senescent Cells Contribute to the Physiological Remodeling of Aged Lungs. *J Gerontol A Biol Sci Med Sci.* 2016;71:153-160. doi: 10.1093/gerona/glu241.

(12) Kamileri I, Karakasilioti I, Sideri, A et al. Defective transcription initiation causes postnatal growth failure in a mouse model of nucleotide excision repair (NER) progeria. *Proc Natl Acad Sci U S A.* 2012;109:2995-3000. doi: 10.1073/pnas.1114941109.

(13) Gackowski D, Starczak M, Zarakowska E, et al. Accurate, Direct, and High-Throughput Analyses of a Broad Spectrum of Endogenously Generated DNA Base Modifications with Isotope-Dilution Two-Dimensional Ultraperformance Liquid Chromatography with Tandem Mass Spectrometry: Possible Clinical Implication. *Anal Chem.* 2016;88:12128-12136. doi: 10.1021/acs.analchem.6b02900.

(14) Ahmad A, Robinson AR, Duensing A, et al. ERCC1-XPF endonuclease facilitates DNA double-strand break repair. *Mol Cell Biol.* 2008;28:5082-5092. doi: 10.1128/MCB.00293-08.

(15) Debacq-Chainiaux F, Erusalimsky JD, Campisi J, Toussaint O. Protocols to detect senescence-associated beta-galactosidase (SA-betagal) activity, a biomarker of senescent cells in culture and in vivo. *Nat Protoc.* 2009;4:1798-1806. doi: 10.1038/nprot.2009.191.

(16) Dimri GP, Lee X, Basile G, et al. A biomarker that identifies senescent human cells in culture and in aging skin in vivo. *Proc Natl Acad Sci U S A.* 1995;92:9363-9367.

(17) Gregg SQ, Robinson AR, Niedernhofer LJ. Physiological consequences of defects in ERCC1-XPF DNA repair endonuclease. *DNA Repair (Amst).* 2011;10:781-791. doi: 10.1016/j.dnarep.2011.04.026.

(18) Wang J, Clauson CL, Robbins PD, Niedernhofer LJ, Wang Y. The oxidative DNA lesions 8,5'-cyclopurines accumulate with aging in a tissue-specific manner. *Aging Cell.* 2012;11:714-716. doi: 10.1111/j.1474-9726.2012.00828.x.

(19) Parrinello S, Samper E, Krtolica A, Goldstein J, Melov S, Campisi J. Oxygen sensitivity severely limits the replicative lifespan of murine fibroblasts. *Nat Cell Biol.* 2003;5:741-747. doi: 10.1038/ncb1024.

(20) van Deursen JM. The role of senescent cells in ageing. *Nature.* 2014;509:439-446. doi: 10.1038/nature13193.

(21) Zhu JK. Active DNA demethylation mediated by DNA glycosylases. *Annu Rev Genet.* 2009;43:143-166. doi: 10.1146/annurev-genet-102108-134205.

(22) Cruickshanks HA, McBryan T, Nelson DM, et al. Senescent cells harbour features of the cancer epigenome. *Nat Cell Biol.* 2013;15:1495-1506. doi: 10.1038/ncb2879.

(23) Nouspikel T, Hanawalt PC. Terminally differentiated human neurons repair transcribed genes but display attenuated global DNA repair and modulation of repair gene expression. *Mol Cell Biol.* 2000;20:1562-1570.

(24) Holliday R. The close relationship between biological aging and age-associated pathologies in humans. *J Gerontol A Biol Sci Med Sci.* 2004;59:B543-B546. doi: 10.1093/gerona/59.6.B543.

(25) Zindy F, Quelle DE, Roussel MF, Sherr CJ. Expression of the p16INK4a tumor suppressor versus other INK4 family members during mouse development and aging. *Oncogene.* 1997;15:203-211. doi: 10.1038/sj.onc.1201178.

(26) Nielsen GP, Stemmer-Rachamimov AO, Shaw J, Roy JE, Koh J, Louis DN. Immunohistochemical survey of p16INK4A expression in normal human adult and infant tissues. *Lab Invest.* 1999;79:1137-1143.

(27) Krishnamurthy J, Ramsey MR, Ligon KL, et al. p16INK4a induces an age-dependent decline in islet regenerative potential. *Nature.* 2006;443:453-457. doi: 10.1038/nature05092.

(28) Ressler S, Bartkova J, Niederegger H, et al. p16INK4A is a robust in vivo biomarker of cellular aging in human skin. *Aging Cell.* 2006;5:379-389. doi: 10.1111/j.1474-9726.2006.00231.x.

(29) Zhu Y, Tchkonia T, Pirtskhalava T, et al. The Achilles' heel of senescent cells: from transcriptome to senolytic drugs. *Aging Cell.* 2015;14:644-658. doi: 10.1111/acel.12344.

(30) Zhu Y, Tchkonia T, Fuhrmann-Stroissnigg H, et al. Identification of a novel senolytic agent, navitoclax, targeting the Bcl-2 family of anti-apoptotic factors. *Aging Cell.* 2016;15:428-435. doi: 10.1111/acel.12445.

(31) Childs BG, Gluscevic M, Baker DJ et al. Senescent cells: an emerging target for diseases of ageing. *Nat Rev Drug Discov.* 2017;16:718-735. doi: 10.1038/nrd.2017.116.

(32) Chen Q, Fischer A, Reagan JD, Yan LJ, Ames BN. Oxidative DNA damage and senescence of human diploid fibroblast cells. *Proc Natl Acad Sci U S A.* 1995;92:4337-4341.

(33) Benayoun BA, Pollina EA, Brunet A. Epigenetic regulation of ageing: linking environmental inputs to genomic stability. *Nat Rev Mol Cell Biol.* 2015;16:593-610. doi: 10.1038/nrm4048.

(34) Bachman M, Uribe-Lewis S, Yang X, Williams M, Murrell A, Balasubramanian S. 5-Hydroxymethylcytosine is a predominantly stable DNA modification. *Nat Chem.* 2014;6:1049-1055. doi: 10.1038/nchem.2064.

(35) Gackowski D, Zarakowska E, Starczak M, Modrzejewska M, Olinski R. Tissue-Specific Differences in DNA Modifications (5-Hydroxymethylcytosine, 5-Formylcytosine, 5-Carboxylcytosine and 5-Hydroxymethyluracil) and Their Interrelationships. *PLoS One.* 2015;10:e0144859. doi: 10.1371/journal.pone.0144859.

(36) Childs BG, Durik M, Baker DJ, van Deursen JM. Cellular senescence in aging and age-related disease: from mechanisms to therapy. *Nat Med.* 2015;21:1424-1435. doi: 10.1038/nm.4000.

(37) Wagner M, Steinbacher J, Kraus TF, et al. Age-dependent levels of 5-methyl-, 5-hydroxymethyl-, and 5-formylcytosine in human and mouse brain tissues. *Angew Chem Int Ed Engl.* 2015;54:12511-12514. doi: 10.1002/anie.201502722.

(38) Ciccarone F, Valentini E, Malavolta M, et al. DNA hydroxymethylation levels are altered in blood cells from Down syndrome persons enrolled in the MARK-AGE project. *J Gerontol A Biol Sci Med Sci.* 2017;00:1-8. doi: 10.1093/gerona/glx198.

(39) Xiong J, Jiang HP, Peng CY, et al. DNA hydroxymethylation age of human blood determined by capillary hydrophilic-interaction liquid chromatography/mass spectrometry. *Clin Epigenetics.* 2015;7:72. doi: 10.1186/s13148-015-0109-x.

(40) Wu H, Zhang Y. Reversing DNA methylation: mechanisms, genomics, and biological functions. *Cell.* 2014;156:45-68. doi: 10.1016/j.cell.2013.12.019.

(41) Spruijt CG, Gnerlich F, Smits AH, et al. Dynamic readers for 5-(hydroxy)methylcytosine and its oxidized derivatives. *Cell.* 2013;152:1146-1159. doi: 10.1016/j.cell.2013.02.004.

(42) Williams K, Christensen J, Pedersen MT, et al. TET1 and hydroxymethylcytosine in transcription and DNA methylation fidelity. *Nature.* 2011;473:343-348. doi: 10.1038/nature10066.

(43) Lu F, Liu Y, Jiang L, Yamaguchi S, Zhang Y. Role of Tet proteins in enhancer activity and telomere elongation. *Genes Dev.* 2014;28:2103-2119. doi: 10.1101/gad.248005.114.

(44) Jin SG, Jiang Y, Qiu R, et al. 5-Hydroxymethylcytosine is strongly depleted in human cancers but its levels do not correlate with IDH1 mutations. *Cancer Res.* 2011;71:7360-7365. doi: 10.1158/0008-5472.CAN-11-2023.

(45) Yang H, Liu Y, Bai F, et al. Tumor development is associated with decrease of TET gene expression and 5-methylcytosine hydroxylation. *Oncogene.* 2013;32:663-669. doi: 10.1038/onc.2012.67.

(46) Chang J, Wang Y, Shao L, et al. Clearance of senescent cells by ABT263 rejuvenates aged hematopoietic stem cells in mice. *Nat Med.* 2016;22:78-83. doi: 10.1038/nm.4010.

(47) Xu W, Yang H, Liu Y, et al. Oncometabolite 2-hydroxyglutarate is a competitive inhibitor of alpha-ketoglutarate-dependent dioxygenases. *Cancer Cell.* 2011;19:17-30. doi: 10.1016/j.ccr.2010.12.014.

(48) Muller T, Gessi M, Waha A et al. Nuclear exclusion of TET1 is associated with loss of 5-hydroxymethylcytosine in IDH1 wild-type gliomas. *Am J Pathol.* 2012;181:675-683. doi: 10.1016/j.ajpath.2012.04.017.

Table 1. The level of epigenetic marks, 5-mdC, 5-hmdC, 5-fdC, as well as 5-hmdU in MEFs, WT and *Ercc1*$^{-/-}$. The data are shown as mean±SD.

	Cells					
Genotype	WT			*Ercc1*$^{-/-}$		
Cell type	Replicative	Quiescent	Senescent	Replicative	Quiescent	Senescent
5-mdC/10^3dN	8.74±0.3075	8.58±0.2795	8.24±0.6610	8.99±0.0525	8.93±0.0251	8.07±0.0661
5-hmdC/10^3dN	0.02±0.0016	0.04±0.0054	0.011±0.0004	0.03±0.0030	0.04±0.0026	0.015±0.0023
5-fdC/10^6dN	0.07±0.0036	0.05±0.0227	0.03±0.0132	0.05±0.0040	0.05±0.0075	0.03±0.0109
5-hmdU/10^6dN	1.52±1.1749	0.91±0.2588	1.04±0.2098	0.72±0.2079	0.58±0.0543	1.14±0.1165

Table 2. The level of epigenetic marks, 5-mdC, 5-hmdC, 5-fdC, 5-cadC as well as 5-hmdU in WT and *Ercc1*$^{-/\Delta}$ livers. The data are shown as mean±SD.

Tissues (livers)					
Genotype	WT			*Ercc1*$^{-/\Delta}$	
Age (weeks)	10	15	130	10	15
5-mdC/10^{3}dN	7.97±0.1836	8.05±0.2240	8.06±0.0346	8.32±0.1709	8.51±0.1688
5-hmdC/10^{3}dN	0.34±0.0175	0.40±0.0162	0.78±0.0058	0.23±0.0072	0.28±0.0055
5-fdC/10^{6}dN	0.22±0.0308	0.23±0.0442	0.24±0.0366	0.14±0.0249	0.19±0.0332
5-cadC/10^{9}dN	5.14±1.0544	5.10±1.3454	4.08±0.9828	3.99±0.8700	4.12±1.2805
5-hmdU/10^{6}dN	0.21±0.0274	0.26±0.0240	0.37±0.0378	0.27±0.0381	0.23±0.0219

Figure 1. DNA repair deficiency promotes cellular senescence

(A) Quantification of expression of senescence markers $p16^{INK4a}$ and $p21^{Cip1}$ mRNA in MEF cultures used for analysis of epigenetic markers.

(B) Quantification of γH2AX foci in WT and *Ercc1*$^{-/-}$ MEFs at passages 3, 5 and 7 grown at 3% or 20% O_2. Cells were fixed and immunostained for γH2AX foci. Ten random fields were analyzed for each cell line and the fraction of cells with foci determined. The average from 3 independent cell lines is plotted on the graph. Error bars represent ±S.E.M. Asterisk indicates significance using a two tailed Student's t-test where $p<0.05$.

(C) Quantification of SA-β-Gal positive cells in WT and *Ercc1*$^{-/-}$ MEF cultures at passage 3, 5 and 7 grown at 3% or 20% O_2. Cells were fixed and stained with X-gal. Ten random fields of view were analyzed for each cell line and the percent of 100-300 cells staining positively for SA-β-Gal determined. The average of 3 independent cell lines is plotted on the graph. Error bars represent the S.E.M. Asterisk indicates significance using a two tailed Student's t-test where $p<0.05$.

(D) Immunoblot detection of the senescence marker $p16^{INK4a}$ in passage 3 WT and *Ercc1*$^{-/-}$ MEFs cultured at 3% or 20% oxygen. β-actin was used as a loading control to calculate the fold-increase in p16 expression relative to WT cells cultured at 3% O_2.

Figure 2. Levels of epigenetic marks in DNA from replicative, quiescent and senescent primary mouse embryonic fibroblasts (MEFs).

(A) Level of 5-mdC.

(B) Level of 5-hmdC.

(C) Level of 5-fdC.

(D) Level of 5-hmdU.

Figure 3. Levels of epigenetic marks in livers DNA of 10-, 15- 130 weeks mice.

(A) Level of 5-mdC.

(B) Level of 5-hmdC.

(C) Level of 5-fdC.

(D) Level of 5-cadC.

(E) Level of 5-hmdU.

Figure 1.

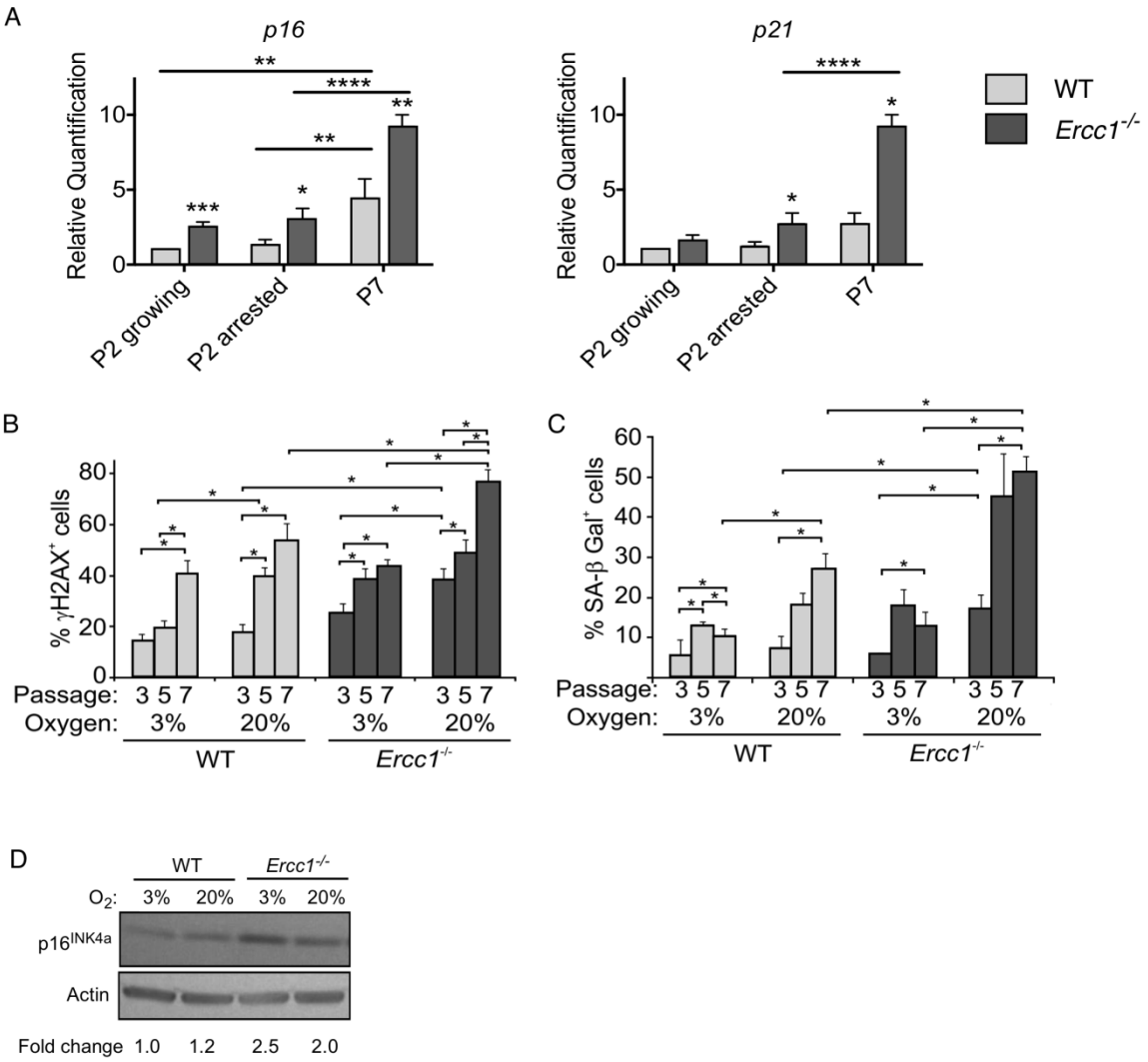

Figure 2.

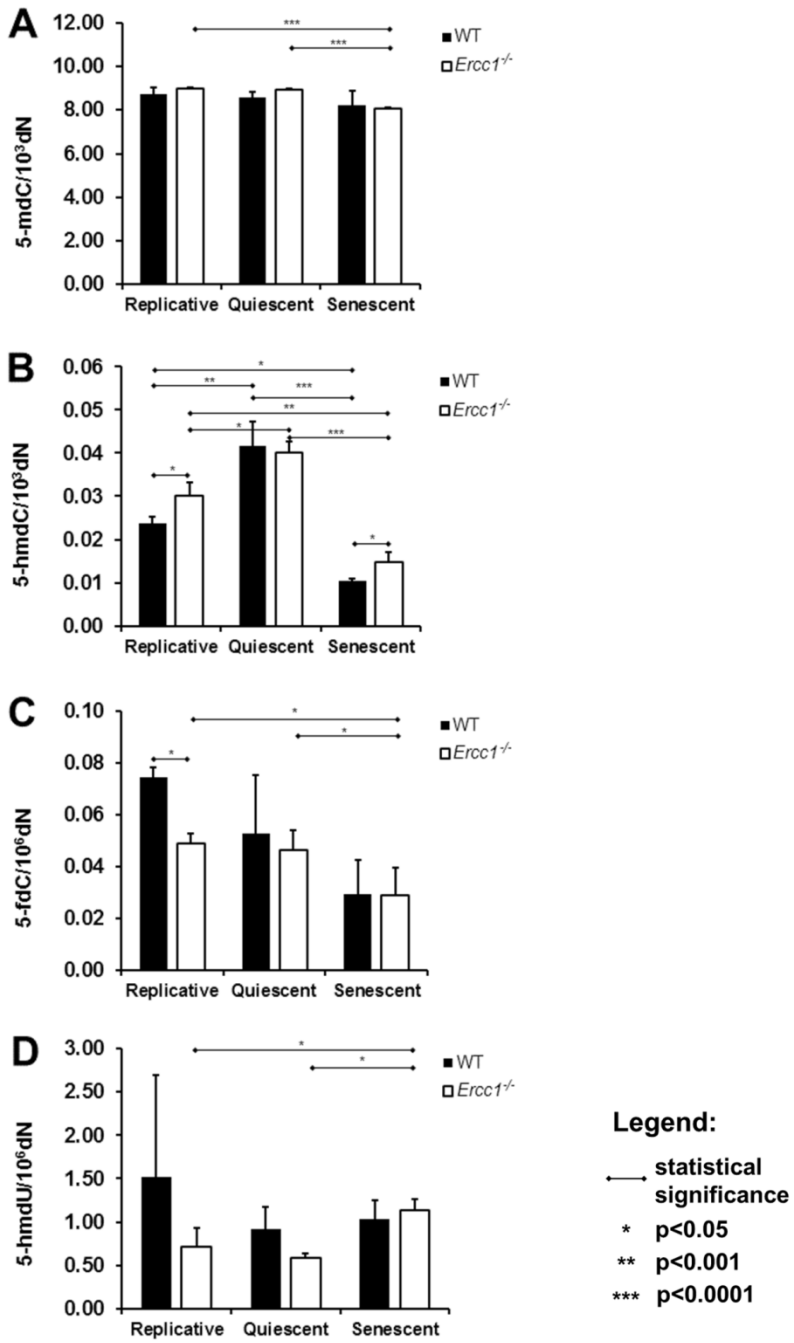

Figure 3.